ISSN 0031-918X, Physics of Metals and Metallography, 2023, Vol. 124, No. 5, pp. 514–519. © Pleiades Publishing, Ltd., 2023.
Russian Text © The Author(s), 2023, published in Fizika Metallov i Metallovedenie, 2023, Vol. 124, No. 5, pp. 428–433.

STRENGTH AND PLASTICITY

On the Precipitation of the Ω-Phase {111} Al Plates in the Al–Cu–Mg Alloy

I. S. Zuiko[a], *, M. R. Gazizov[a], and R. O. Kaibyshev[a]

[a] *Belgorod State University, Belgorod, 308015 Russia*

**e-mail: zuiko_ivan@bsu.edu.ru*

Received November 29, 2022; revised March 13, 2023; accepted March 15, 2023

Abstract—The precipitation of Ω-phase $\{111\}_\alpha$ plates in the Al–Cu–Mg alloy has been investigated at a Cu/Mg ratio > 10 and low Si content. Unlike Al–Cu–Mg alloys containing Ag, nanoscale plates with an $\{111\}_\alpha$ habit plane has been found for the first time to precipitate in the alloy according to a heterogeneous mechanism, namely, along low-angle boundaries, dislocation lines, and at the θ'-phase/Al-matrix interphase boundary.

Keywords: phase transformations, strengthening particles, aging, thermally hardened alloy, heterogeneous precipitation

DOI: 10.1134/S0031918X23600409

INTRODUCTION

One of the basic concepts of modern materials science is the formation of a desired microstructure in a material, which depends on its chemical composition and processing conditions. Therefore, heat-hardenable aluminum alloys are a commercially important group of materials, since their properties can be improved by selecting optimal processing conditions [1].

Microalloying is well known to improve the operational characteristics of alloys. For example, Mg additives increase the strength, plasticity, and heat resistance of an Al–Cu alloy [1]. However, despite the fact that the first duralumin (Al–Cu–Mg alloy) was discovered more than a century ago, scientists are still discussing the mechanisms of precipitation of strengthening elements, such as clusters, zones, and phases, and their interaction with dislocations.

The phase compositions and properties of binary Al–Cu alloys are well described in the literature, since they are the basis for a wide class of heat-hardenable alloys (the 2xxx series according to the Aluminum Association). Therefore, here, we consider compositions with small additions of Mg and other elements that affect the type and structure of hardening phases. Quenching of these alloys results in a supersaturated solid solution (SSS) of alloying elements, which decomposes to form clusters, zones, or phases upon subsequent heating or aging. The traditional treatment of these alloys is heat treatment (HT), which includes hardening and aging. Low-temperature thermomechanical treatment (LTTT), which includes cold plastic deformation performed prior to aging, is also used to significantly improve strength as compared to HT.

The sequence of phase transformations in Al–Cu–Mg alloys with Cu/Mg ≥ 5.6 as a result of SSS decomposition has the following form:

$$\begin{aligned}\mathrm{SSS} \to \{001\}\ \text{clusters} \to \text{GP zones}\ (\mathrm{Al_3Cu})\\ \to \text{GP zones} + \theta''(\mathrm{Al_3Cu}) \to \theta'' + \theta'(\mathrm{Al_2Cu})\\ \to \theta' \to \theta(\mathrm{Al_2Cu});\end{aligned} \quad (1)$$

$$\begin{aligned}\mathrm{SSS} \to \{111\}\ \text{clusters} \to \Omega(\mathrm{Al_2Cu})\\ \to \theta \to \sigma(\mathrm{Al_5Cu_6Mg_2}).\end{aligned} \quad (2)$$

Reactions (1) and (2) proceed on the matrix planes $\{001\}_\alpha$ and $\{111\}_\alpha$, respectively. The Guinier–Preston (GP) zones, θ" and θ' phases have been considered in previous works [2, 3]. In this paper, we consider Ω-phase particles in detail.

Another example of microalloying is the addition of Ag to Al–Cu–Mg alloys. These compositions are characterized by strength and creep resistance because silver provides a homogeneous precipitation of Ω-phase plates [1, 4–10]. Its particles have a high resistance to coarsening at elevated temperatures (up to 200°C), which can be explained by the segregation of magnesium and silver at its wide boundaries [1].

Despite intensive research, the exact crystal lattice of the Ω phase is still a matter of debate. This phase is represented in the literature as a form of stable θ phase with nominal Al_2Cu stoichiometry [7, 10, 11]. It belongs to the *Fmmm* space group (a = 0.496 nm, b = 0.859 nm, c = 0.848 nm) [12]. The orientation ratio is one of 22 possible ratios for equilibrium θ-Al_2Cu: $(111)_\alpha \| (001)_\Omega$ and $[10\bar{1}]_\alpha \| [010]_\Omega$, and $[1\bar{2}1]_\alpha \| [100]_\Omega$ [4, 8, 12]. Given that the mismatch between the lat-

tices of the Ω phase and matrix in the habit plane is less than 0.0015%, their particles are coherent along $\{111\}_\alpha$ planes. The mismatch parameter around the plate butts in the ⟨111⟩ direction along the c axis is ~9.3% [1]. Complete matching along $\{111\}_\alpha$ planes occurs due to the segregation of Ag and Mg atoms and, possibly, vacancies [7, 13]. A driving force for the segregation of Mg and Ag is a decrease in the mismatch between the matrix and particles [7]. The kinetics of the growth of Ω particles in alloys with and without silver is noted to differ significantly [14].

In addition, the excellent resistance of the Ω phase to coarsening is associated with the high energy barrier of step nucleation in the strong vacancy field that is normal to the flat interphase boundary of the plate [15]. The precipitation of Ω particles in Al–2.5Cu–1.5Mg–0.5Ag was first reported in the 1970s [12], but this fact has not gained sufficient attention. Many works [10] later focused on these plates, but it was demonstrated only in 1990 that they could also precipitate in alloys containing no silver. The interval of more than a quarter of a century between these events can be explained by the high silicon content in early Al–Cu–Mg alloys [6]. The binding energy between Si and Mg atoms is known to be higher than that between Ag and Mg. This causes predominant formation of Mg–Si clusters at the early stages of aging and suppresses the precipitation of Ag–Mg clusters, which are possible precursors of the Ω phase. An Al–Cu alloy must contain at least 0.1–0.3 wt % Mg (Si/Mg > 2) for Ω particles to be present in the structure [6, 13] and for the mechanical properties to be significantly improved.

Ag/Mg additives decrease the intensity of diffuse $\{002\}_\alpha$ strands (rods) in electron diffraction patterns, indicating a decrease in the number of Guinier–Preston zones [16]. Zn atoms are also known to be present in Al–Cu–Mg–Ag alloys along the flat interphase boundaries of Ω-phase plates (at the sites initially occupied by Ag) [17].

As previously mentioned, Ag is not a necessary element for alloying the Ω-phase [4] and has almost no effect on the aging of binary Al–Cu and Al–Mg alloys, but it intensifies the aging effect in ternary Al–Cu–Mg alloys [1] and reduces the time for reaching maximum strength/hardness. In analyzing the scientific literature we revealed the following possible mechanisms of Ω-phase evolution in Ag-free Al–Cu–Mg alloys:

(1) The authors of [18] showed that during sliding, dislocations capture dissolved atoms of alloying elements from solid solution using fast diffusion along the core, therefore particles can nucleate at dislocations. For example, Mg–Cu precursors were detected along a dislocation by STEM-HAADF [19] and 3D atomic tomography [14]. The formation of these precursors can be attributed to the strong Mg–Cu interaction at dislocations; however, some dissolved Mg and Cu atoms are also found at dislocations [14]. Hypothetically, these structures could be precursors for $\{111\}_\alpha$ particles. In addition, positron annihilation showed complexes containing Mg–Cu vacancies in the vicinity of vacancy sinks, i.e., dislocations [20].

(2) Direct lattice resolution showed that tiny (less than 12 atoms) lamellar copper clusters can be detected on close-packed $\{111\}_\alpha$ planes in the standard Al–4% Cu alloy during the initial stages of aging [21]. These precipitates are unstable after 10 hours of aging at 100°C, namely, they grow and dissolve even when exposed to an electron microscope beam. Similar precipitations were detected in Al–1.0Si–0.5Cu [22] and Al–Cu–Mg [11] thin films. The authors of these works detected nano-scale lamellar GP zones with a unconventional $\{111\}_\alpha$ habit plane.

(3) Only magnesium clusters are probably the sites of heterogeneous nucleation of the Ω phase [6].

The addition of Cu to Al either weakly or does not change the stacking fault energy (which determines the tendency of a material to cross-slip dislocations) [23], but Ag and Mg reduce it enough to promote dislocation splitting and accommodation of dissolved element atoms on close-packed $\{111\}_\alpha$ planes [7, 19, 23], on which the Ω phase can nucleate. This explains the accelerated formation of GP zones on $\{111\}_\alpha$ planes along with the traditional $\{001\}_\alpha$ [11]. In this regard, N. Sano et al. assumed [13] that Ag additives increase the density of {111} stacking faults, which act as sites of heterogeneous particle nucleation.

Finally, we can conclude that the nature of Ω-phase precipitation is not reliably known, despite the extensive number of studies on the phase composition evolution of Al–Cu–Mg alloys during aging. This work aims to investigate the preferred sites of the nucleation and growth of $\{111\}_\alpha$ Ω-phase plates in a silver-free Al–Cu–Mg alloy (modern high-strength alloy AA2519) using transmission electron microscopy. The results of the study can be useful for the development of new alloys and the optimization of HT/TMT treatments of Al–Cu–Mg alloys to precipitate desired phases.

EXPERIMENTAL

The material for the study was the AA2519 alloy with a chemical composition of Al–5.64 Cu–0.33 Mn–0.23 Mg–0.15 Zr–0.11 Ti–0.09 V–0.08 Fe–0.08 Zn–0.04 Sn–0.01 Si(wt %), which was prepared by semicontinuous casting at Belgorod State University. After homogenizing annealing (510°C, 24 h) ingots were forged ($\varepsilon_{true} \approx 2.0$) and rolled ($\varepsilon_{true} \approx 1.4$) at $T = 425$°C. Samples were cut from hot-rolled plates, hardened at $T = 525$°C for 1 hours, quenched in cold water (20°C), and aged for 5 hours at 180°C (maximum strength state [24]).

To study the morphology of dispersed particles of the secondary phases, we prepared thin foils from the

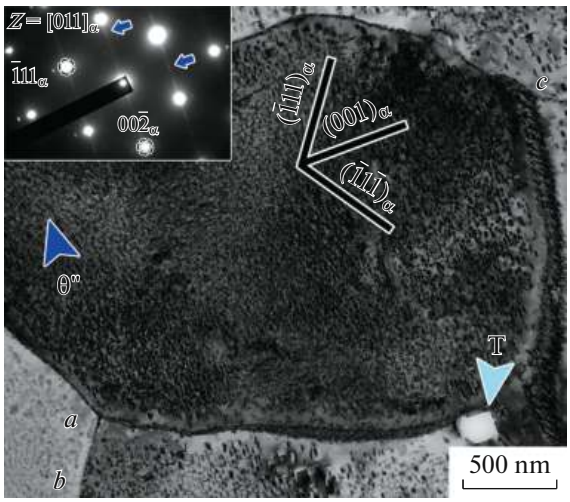

Fig. 1. The microstructure of the AA2519 alloy after ageing for maximum strength. The regions shown in Fig. 2 are indicated by the letters *a*, *b*, and *c*.

treated alloy using standard electropolishing in a 25% HNO_3 + 75% CH_3OH solution cooled to −30°C on the Struers TenuPol-5 device at 20 V.

Transmission electron microscopy was performed using a JEOL JEM-2100 microscope at an accelerating voltage of 200 kV. All other details of the experiment, including the electron diffraction patterns of the studied alloy, were described in previous papers [2, 3, 24].

RESULTS AND DISCUSSION

Figure 1 shows the microstructure of the alloy after aging for maximum strength. Given the habit plane of Ω particles, the image was taken when the electron beam was oriented strictly parallel to the $\langle 011\rangle_\alpha$ direction. As expected, analysis of the electron diffraction patterns of the central region (inset in Fig. 1) indicates that uniformly distributed θ"-phase particles (indicated by the blue arrow) dominate in the structure. This is evidenced by distinct discontinuous diffuse strands along $\langle 002\rangle_\alpha$ (inset in Fig. 1). EDXS analysis [24] also detected a dispersoid of the *T*-$Al_{20}Cu_2Mn_3$ phase (indicated by a blue arrow). However, no Ω plates were detected at the *T*-phase/matrix interphase boundary in contrast to those found in Al–Cu–Mg–Ag alloys [10].

In the first approximation, the intensity of diffraction effects (reflections, strands) is proportional to the volume fraction of the particles. No reflections typical of Ω particles at positions 1/3 and 2/3 [220]α and diffuse strands along $\langle 111\rangle_\alpha$ were detected. Therefore, we can assume that its volume fraction in this state is small, but it increases during low-temperature thermomechanical treatment [3]. These observations are in complete agreement with previous results [3, 25].

The mechanical properties of alloys are known [1] to depend not only on the volume fraction of the secondary phases, but also on the complex of their morphological features, such as size, shape, density of precipitation, spatial distribution, and coherence. There is no consensus according to which particles (with a $\{111\}_\alpha$ or $\{001\}_\alpha$ habit plane) are the most effective in preventing dislocations from sliding during plastic deformation [26]. The precipitation of particles on only one type of matrix plane has been found to result in low fracture toughness [1]. Given that the dominant slip in FCC crystals (Al) occurs in the primary slip $\langle 110\rangle_{Al}$ $\{111\}_{Al}$ system along close-packed {111} atomic planes (main slip planes), Al–Cu–Mg–Ag alloys hardened with $\{111\}_{Al}$ Ω-phase plates exhibit a higher strength even though the shear stresses of both plate types (θ' and Ω) are approximately the same [26].

Figure 2 shows the regions indicated by the letters in Fig. 1. Taking the planes of location into account, it is quite easy to identify θ"/θ' and Ω plates. Figures 2a and 2b show that $\{111\}_\alpha$ Ω-phase plates precipitate at low-angle boundaries. The misorientation of the boundary can be indirectly estimated from the contrast of the images (see Fig. 1). The exact angle of boundary misorientation in this section was not found by the Kikuchi-line identification method, but analysis of electron diffraction patterns (not presented) taken from the boundary and regions from both sides of the boundary revealed that the angle of rotation was less than 10°. Therefore, we can assume that the boundary is low-angle.

The precipitation of Ω plates at θ' particles was also detected (Fig. 2c). The typical point-like electron diffraction, specific contrast, and plate widths indicate that this is a semicoherent phase rather than a coherent θ" phase [2, 3, 25]. Figure 2a also shows a θ' particle with increased thickness at the high-angle boundary (indicated by the green arrow). Previously, heterogeneous precipitation of θ' at lattice imperfections, such as dislocations, boundaries with a misorientation of at least 8°–12°, and at interphase boundaries have been reported [17, 26].

To demonstrate that this is not a single case of particle precipitation at boundaries, Fig. 3 shows another section. As in the previous case, coherent θ' plates precipitate homogeneously in the matrix and θ' and Ω particles precipitate at low-angle boundaries. There are a number of precipitation-free zones along boundaries. This phenomenon is typical of grain boundaries in thermally hardenable alloys after quenching and aging treatments [1].

The phase composition study revealed that θ' and Ω plates can precipitate not only in the grain body and at low-angle boundaries, but also along dislocation lines. Figure 4 illustrates this. There are strands (indicated by red arrows) along $\langle 111\rangle_\alpha$ in the diffraction pattern (inset in Fig. 4b), which is a distinctive feature of thin Ω-phase plates [3, 5]. However, it is difficult to

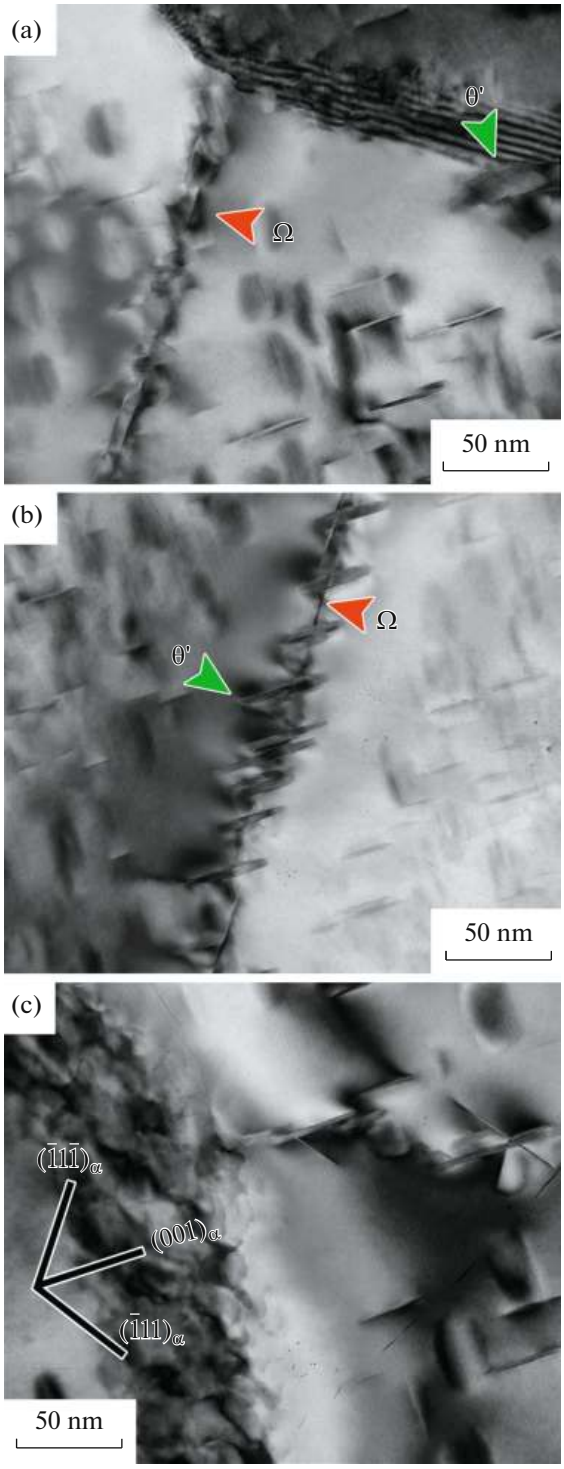

Fig. 2. TEM images showing heterogeneous precipitation of Ω particles. Images (a), (b), and (c) were taken from the places indicated by the corresponding letters in Fig. 1.

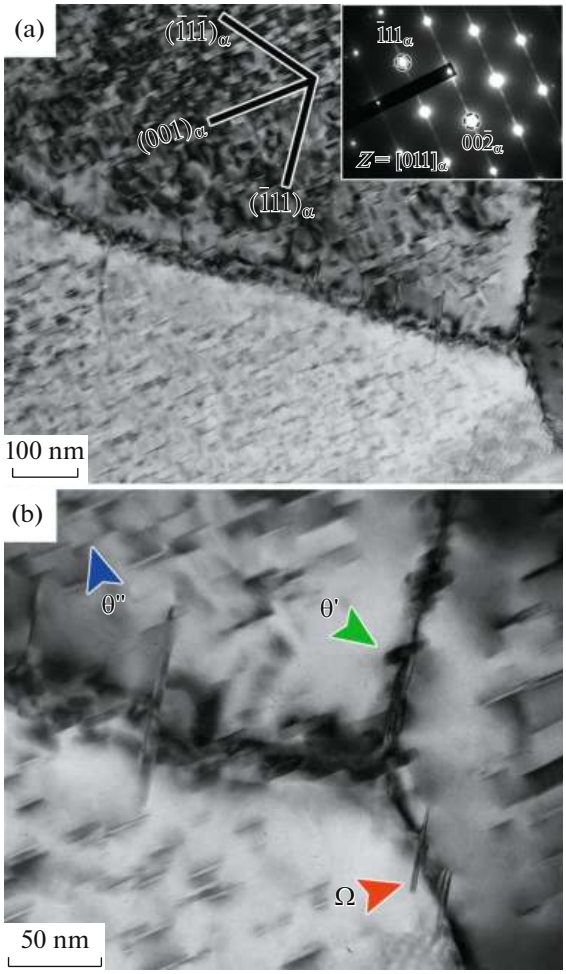

Fig. 3. The alloy microstructure with heterogeneous precipitation of θ' and Ω particles. Zone axis $\langle 011 \rangle_\alpha$. (b) is an enlarged image of the structure shown in Fig. 3a.

detect typical point reflections, which is due to the small amount of the phase in this state. The assumption that Ω particles precipitate at dislocations could not be confirmed after careful examination of the TEM images. However, this mechanism has been detected for $\{111\}_\alpha$ particles of the T_1 phase (Al_2CuLi) in Al–Cu–Li alloys [27]. It is interesting to note that the T_1 and Ω phases are isostructural, namely, the electron diffraction patterns are absolutely the same and Ag atoms also segregate at the particle/matrix interphase boundary.

The authors tend to believe that small Ω particles form around θ' particles, which were initially precipitated at a dislocation, or within elastic stress fields surrounding a dislocation line. We believe that the more probable scenario is heterogeneous nucleation of the Ω phase at the Cottrell atmospheres, which are formed by sliding dislocations. Oscillations (Portevin–Le Chatelier effect) on the tensile curves of the quenched alloy indicate the presence of these regions with an increased concentration of interstitial atoms [3]. However, further research in this direction is needed.

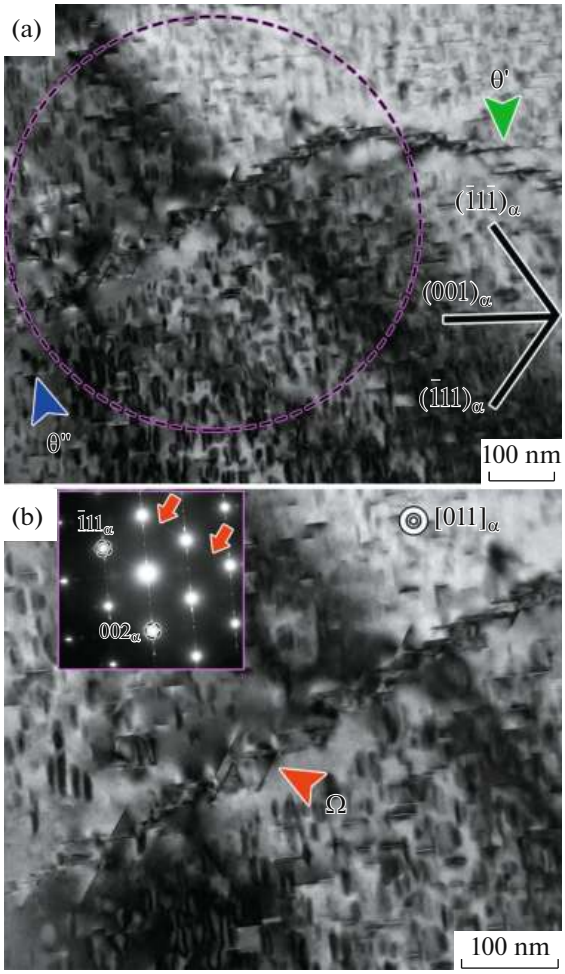

Fig. 4. The microstructure of the internal grain volumes in the alloy. The position and the size of the selector aperture (∅0.64 μm) used to obtain the electron difraction pattern is indicated by the dotted line. (b) is an enlarged image of the structure shown in Fig. 4a.

CONCLUSIONS

In this work, we determined the sites for heterogeneous precipitation of Ω-phase particles in the modern high-strength Al–Cu–Mg alloy (AA2519). We demonstrated that particles with a $\{111\}_\alpha$ habit plane can precipitate not only near the dislocation line, but also at low-angle and θ'-phase/Al-matrix interphase boundaries. We believe that it is necessary to continue the investigation of Ω-phase nucleation sites at the atomic level using 3D atomic tomography and/or direct resolution scanning microscopy to determine the exact location of some atoms and their clusters (possibly Cu–Mg clusters near the dislocation line along the $\langle 111\rangle_\alpha$ directions).

FUNDING

This work was supported by the grant of the Belgorod State University (Young Leaders in Science within the framework of the Science of the 21st century project of the Priority-2030 program).

CONFLICT OF INTEREST

The authors declare that they have no conflicts of interest.

REFERENCES

1. I. Polmear, D. StJohn, J.-F. Nie, and M. Qian, *The Light Metals: Metallurgy of the Light Metals*, 5th ed. (Elsevier, 2017). https://doi.org/10.1016/B978-0-08-099431-4.00009-9
2. I. Zuiko and R. Kaibyshev, "Aging behavior of an Al–Cu–Mg alloy," J. Alloys Compd. **759**, 108–119 (2018). https://doi.org/10.1016/j.jallcom.2018.05.053
3. I. Zuiko and R. Kaibyshev, "Effect of plastic deformation on the ageing behaviour of an Al–Cu–Mg alloy with a high Cu/Mg ratio," Mater. Sci. Eng., A **737**, 401–412 (2018). https://doi.org/10.1016/j.msea.2018.09.017
4. S. C. Wang and M. J. Starink, "Precipitates and intermetallic phases in precipitation hardening Al–Cu–Mg–(Li) based alloys," Int. Mater. Rev. **50**, 193–215 (2005). https://doi.org/10.1179/174328005x14357
5. M. Gazizov and R. Kaibyshev, "Effect of pre-straining on the aging behavior and mechanical properties of an Al–Cu–Mg–Ag alloy," Mater. Sci. Eng., A **625**, 119–130 (2015). https://doi.org/10.1016/j.msea.2014.11.094
6. B. M. Gable, G. J. Shiflet, and E. A. Starke, "The effect of Si additions on Ω precipitation in Al–Cu–Mg–(Ag) alloys," Scr. Mater. **50**, 149–153 (2004). https://doi.org/10.1016/j.scriptamat.2003.09.004
7. L. Reich, M. Murayama, and K. Hono, "Evolution of Ω phase in an Al–Cu–Mg–Ag alloy—A three-dimensional atom probe study," Acta Mater. **46**, 6053–6062 (1998). https://doi.org/10.1016/s1359-6454(98)00280-8
8. R. Yoshimura, T. J. Konno, E. Abe, and K. Hiraga, "Transmission electron microscopy study of the evolution of precipitates in aged Al–Li–Cu alloys: The θ' and T1 phases," Acta Mater. **51**, 4251–4266 (2003). https://doi.org/10.1016/s1359-6454(03)00253-2
9. R. Yoshimura, T. J. Konno, E. Abe, and K. Hiraga, "Transmission electron microscopy study of the early stage of precipitates in aged Al–Li–Cu alloys," Acta Mater. **51**, 2891–2903 (2003). https://doi.org/10.1016/s1359-6454(03)00104-6
10. A. K. Mukhopadhyay, "Coprecipitation of Ω and σ phases in Al–Cu–Mg–Mn alloys containing Ag and Si," Metall. Mater. Trans. A **33**, 3635–3648 (2002). https://doi.org/10.1007/s11661-002-0238-7
11. S. Mondol, T. Alam, R. Banerjee, S. Kumar, and K. Chattopadhyay, "Development of a high temperature high strength Al alloy by addition of small amounts of Sc and Mg to 2219 alloy," Mater. Sci. Eng., A **687**, 221–231 (2017). https://doi.org/10.1016/j.msea.2017.01.037
12. J. H. Auld, J. T. Vietz, and I. J. Polmear, "T-phase precipitation induced by the addition of silver to an alu-

minium–copper–magnesium alloy," Nature **209**, 703–704 (1966). https://doi.org/10.1038/209703a0

13. N. Sano, K. Hono, T. Sakurai, and K. Hirano, "Atom-probe analysis of Ω and θ' phases in an Al–Cu–Mg–Ag alloy," Scr. Metall. Mater. **25**, 491–496 (1991). https://doi.org/10.1016/0956-716X(91)90216-N
14. V. Araullo-Peters, B. Gault, F. de Geuser, A. Deschamps, and J. M. Cairney, "Microstructural evolution during ageing of Al–Cu–Li–*x* alloys," Acta. Mater. **66**, 199–208 (2014). https://doi.org/10.1016/j.actamat.2013.12.001
15. M. R. Gazizov, A. O. Boev, C. D. Marioara, R. Holmestad, D. A. Aksyonov, M. Yu. Gazizova, and R. O. Kaibyshev, "Precipitate/matrix incompatibilities related to the {111}Al Ω plates in an Al–Cu–Mg–Ag alloy," Mater. Charact. **182**, 111586 (2021). https://doi.org/10.1016/j.matchar.2021.111586
16. R. Ferragut, A. Dupasquier, C. E. Macchi, A. Somoza, R. N. Lumley, and I. J. Polmear, "Vacancy–solute interactions during multiple-step ageing of an Al–Cu–Mg–Ag alloy," Scr. Mater. **60**, 137–140 (2009). https://doi.org/10.1016/j.scriptamat.2008.09.011
17. S. Wenner, C. D. Marioara, S. J. Andersen, M. Ervik, and R. Holmestad, "A hybrid aluminium alloy and its zoo of interacting nano-precipitates," Mater. Charact. **106**, 226–231 (2015). https://doi.org/10.1016/j.matchar.2015.06.002
18. U. Dahmen and K. H. Westmacott, "The mechanism of φ' precipitation on climbing dislocations in Al–Cu," Scr. Metall. **17**, 1241–1246 (1983). https://doi.org/10.1016/0036-9748(83)90292-2
19. E. Gumbmann, W. Lefebvre, F. De Geuser, C. Sigli, and A. Deschamps, "The effect of minor solute additions on the precipitation path of an Al Cu Li alloy," Acta Mater. **115**, 104–114 (2001). https://doi.org/10.1016/j.actamat.2016.05.050
20. Y. Nagai, M. Murayama, Z. Tang, T. Nonaka, K. Hono, and M. Hasegawa, "Role of vacancy–solute complex in the initial rapid age hardening in an Al–Cu–Mg alloy," Acta Mater. **49**, 913–920 (2001). https://doi.org/10.1016/S1359-6454(00)00348-7
21. H. Yoshida, H. Hashimoto, Ya. Yokota, and N. Ajika, "High resolution lattice images of G.P. zones in an Al–3.97 wt % Cu alloy," Trans. Jpn. Inst. Met. **24**, 378–385 (1997). https://doi.org/10.2320/matertrans1960.24.378
22. Ch.-H. Tung, R.-L. Chiu, and P.-H. Chang, "Observations of Guinier–Preston zones in an as-deposited Al–1 wt % Si–0.5 wt % Cu thin film," Scr. Mater **24**, 1473–1477 (1996). https://doi.org/10.1016/1359-6462(96)00004-8
23. P. Ying, Z. Liu, S. Bai, M. Liu, L. Lin, P. Xia, and L. Xia, "Effects of pre-strain on Cu–Mg co-clustering and mechanical behavior in a naturally aged Al–Cu–Mg alloy," Mater. Sci. Eng.: A **704**, 18–24 (2016). https://doi.org/10.1016/j.msea.2017.06.097
24. I. S. Zuiko, S. Mironov, S. Betsofen, and R. Kaibyshev, "Suppression of abnormal grain growth in friction-stir welded Al–Cu–Mg alloy by lowering of welding temperature," Scr. Mater. **196**, 113765 (2021). https://doi.org/10.1016/j.scriptamat.2021.113765
25. I. S. Zuiko, M. R. Gazizov, and R. O. Kaibyshev, "Effect of thermomechanical treatment on the microstructure, phase composition, and mechanical properties of Al–Cu–Mn–Mg–Zr alloy," Phys. Met. Metallogr. **117**, 906–919 (2016). https://doi.org/10.1134/S0031918X16090088
26. B. M. Gable, A. W. Zhu, A. A. Csontos, and E. A. Starke, "The role of plastic deformation on the competitive microstructural evolution and mechanical properties of a novel Al–Li–Cu–*X* alloy," J. Light Met. **1**, 1–14 (2001). https://doi.org/10.1016/s1471-5317(00)00002-x
27. W. A. Cassada, G. J. Shiflet, and E. A. Starke, "Mechanism of Al_2CuLi (T1) nucleation and growth," Metall. Trans. A **22**, 287–297 (1991). https://doi.org/10.1016/S1471-5317(00)00002

Translated by T. Gapontseva